三电极高速 CO_2 双边角焊工艺参数对焊缝成形影响

马晓丽[1]，　华学明[1]，　林　航[1]，　吴毅雄[1]，
鬼木保彦[2]，　上藤茂[2]，　施建刚[2]
（1. 上海交通大学 上海市激光制造与材料表面改性重点实验室，上海　200240；
2. 日本常石造船株式会社，广岛　7200393）

马晓丽

摘　要：在传统双电极角焊焊接工艺基础上，为了进一步提高焊接效率，采用三电极高速 CO_2 双边角焊工艺，分析不同焊接工艺参数对焊缝成形参数的影响. 结果表明，采用不同极性组合的焊缝成形参数差别不大；随着速度的减慢和焊接工艺参数的增大，脚长、熔深和熔宽均呈增大趋势，但焊脚长度有一个最大值限制. 下脚长、上脚长受中间焊枪的指向位置影响更为明显，当左右两侧焊枪对中时，脚长最小. 另外，随着焊丝之间距离的增大，脚长和熔宽逐渐减小，余高随焊丝距离增大而增大，但差别不大.

关键词：三电极高速 CO_2 双边角焊；极性组合；左右侧焊枪偏移量；焊缝成形参数
中图分类号：TG444　　文献标识码：A　　文章编号：0253－360X(2009)10－0093－04

0　序　　言

为了提高中国工业企业的焊接生产效率和焊接技术水平，在船舶气体保护电弧焊接领域中，国内普遍采用多电极的弧焊技术，采用多焊枪施焊，每个焊枪配一路焊丝，每路焊丝都有自己的电源、送丝机构和调节系统. 这样每根焊丝的电弧电压和送丝速度可分别作不同的调节. 基本出发点是在提高焊接速度的同时提高各个电极的焊接电流，以维持焊接热输入大体上保持不变. 最常见的高速焊接以 CO_2 作为保护气体.

国内的造船企业双电极焊接平面分段流水线，通常焊接速度可达 1.2 m/min[1]. 主要用于钢板平面组装阶段的船体平行中体外板、双层底板、顶板、甲板隔壁等的拼板对接焊，以及相应结构的焊接. 虽然这些在船厂的生产中发挥了较大的作用，但都通常必须依靠进口，故在国内创立自主更为高效的多电极焊接工艺流水线势在必行.

目前对于三电极以上的熔化极气体保护焊接技术研究还很罕见. 文中分析了两种极性组合对比、焊接电流速度匹配、焊枪指向、左右两侧焊枪偏移量和焊枪之间距离等不同的焊接参数对三电极高速 CO_2 双边角焊的焊缝成形影响.

收稿日期：2008－07－17

1　试验方法

1.1　试验设备与材料

试验利用三电极双边角焊高速焊接系统，对 15 mm 厚的底板，12 mm 厚的肋板的船用 AB-A 级钢板进行双边角焊试验. 保护气体为 100%CO_2，流量为 22 L/min，焊丝牌号为 MX-200H，直径为 1.6 mm. 每侧 3 把焊枪分别有独立的焊机和各自的送丝系统. 两侧沿焊接方向依次为引导弧、中间弧和跟随弧，各三弧设计成一直线，可以作相对的偏移微调，且具有相同转动轴调整转角以调节熔池的流动行为，试验可以通过调节每侧的焊接工艺参数、焊丝之间距离、焊枪之间夹角、倾角和焊枪指向等参数获得理想的焊缝成形. 具体的空间位置参数如图 1 所示，其中－3～2 mm是指焊枪的指向量，负号表示焊枪指向

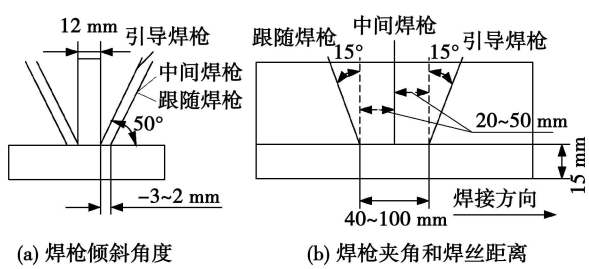

(a) 焊枪倾斜角度　　(b) 焊枪夹角和焊丝距离

图 1　三电极高速 CO_2 双边角焊空间位置示意图
Fig. 1　Schematic of triple-electrode CO_2 welding

肋板位置.

1.2 试验设备与材料

为了研究三电极双边角焊在焊接效率、焊缝成形等方面的优势,主要基于以往三电极单边角焊的试验研究基础[2,3],进行了极性组合试验(DCEP/DCEN/DCEP 和 DCEN/DCEP/DCEN,其中 DCEP 表示直流正接,DCEN 表示直流反接,为了简便起见,DCEP/DCEN/DCEP 简称 PNP,DCEN/DCEP/DCEN 简称 NPN),按 3 把焊枪的电流相对大小设计了大中小、大中中、大小中、大大中和大中大 5 种电流组合,如表 1 所示,焊接速度为 1.8 m/min. 在此基础上,选用 460/360/360 A,400/300/300 A 和 340/240/240 A 电流组合与焊接速度分别为 1.4,1.6,1.8 m/min 进行匹配试验. 进行了引导焊枪为焊缝中心,中间焊枪和跟随焊枪分别为纵向 2 mm,横向 1 mm 和 3 mm 的焊枪指向试验;焊枪左右偏移量分别为左前 60 mm,左前 30 mm,左右对中,右前 30 mm,右前 60 mm 的焊枪偏移量试验;焊丝之间距离分别为 20,30,40,50 mm 的试验. 在焊枪指向试验、偏移量试验和焊丝距离试验中,焊接速度为 1.6 m/min,右侧焊枪在前 30 mm.

表 1 NPN 和 PNP 极性组合的焊接工艺参数

Table 1 Weld parameters of combination of NPN and PNP

电流参数组合	引导电极		中间电极		跟随电极	
	电流 I/A	电压 U/V	电流 I/A	电压 U/V	电流 I/A	电压 U/V
大中小	450	39.6	350	34.6	300	32.0
	450	39.6	300	32.0	250	29.6
	400	37.0	300	32.0	250	29.6
大中中	450	39.6	350	34.6	350	34.6
	400	37.0	300	32.0	300	32.0
	350	34.6	300	32.0	300	32.0
大小中	450	39.6	350	34.6	400	37.0
	450	39.6	300	32.0	350	34.6
	400	37.0	300	32.0	350	34.6
大大中	450	39.6	450	39.6	300	32.0
	400	37.0	400	37.0	300	32.0
	350	34.6	350	34.6	300	32.0
大中大	400	37.0	350	34.6	400	37.0
	400	37.0	300	32.0	400	37.0
	350	34.6	300	32.0	350	34.6

2 试验结果及分析

试验分析了不同焊接工艺参数对焊缝成形参数的影响. PNP 极性组合与 NPN 极性组合的脚长平均值均为 6 mm 左右,故可认为两种极性焊接时焊缝成形参数差别不大,且脚长和熔宽的变化趋势相同,如图 2 所示.

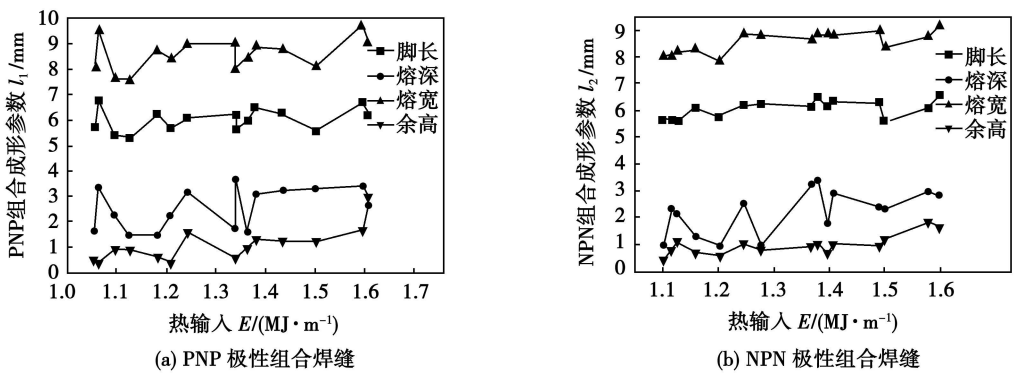

(a) PNP 极性组合焊缝 (b) NPN 极性组合焊缝

图 2 PNP 极性与 NPN 极性组合时热输入与焊缝成形参数关系

Fig. 2 Relationship between heat input and weld geometry parameters with PNP and NPN combinations

图3所示为焊接速度组合试验与焊缝成形参数的关系，可知随着速度的减慢和焊接工艺参数组合的增大，脚长、熔深和熔宽均呈增大趋势．在提高焊接速度的同时采用较大的焊接电流来增大沿焊接方向上的热源长度．随热源沿焊接方向上的拉长，焊道最宽处的熔宽增大，且由于高速焊接而造成的最宽处的熔宽减小的程度降低，这样可有利地防止咬边、驼峰缺陷的产生，这也正是采用三电极高速MAG双边角焊焊接方法的出发点．另外，高速角焊时焊脚长度有一个最大值限制，此时无论怎样增大电流或怎样减小速度来增大熔敷率，都无法得到满意的焊缝．只有焊脚长度和熔敷金属量满足一定的匹配条件时，才能获得良好的焊缝，当熔敷金属过多或焊脚长度过小时，在接头的水平板上出现焊道满溢的现象．而熔敷金属过少或焊脚长度过大时，在接头的垂直板上出现咬边，严重时出现驼峰[4,5]．

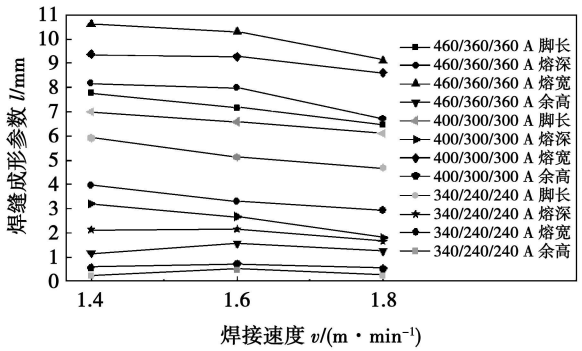

图3　焊接速度组合与焊缝成形参数的关系

Fig. 3　Relationship between welding speed combination and weld geometry parameters

由焊枪指向试验可以看出：下脚长、上脚长受中间焊枪的指向位置影响更为明显．下脚长随水平指向的增大而增大，上脚长随纵向指向的增大而增大，如图4所示，负号表示焊枪指向纵向位置．焊枪指向位置对熔深、熔宽和余高的影响并不显著，由于篇幅限制，在此不做具体的图表说明．另外，焊枪指向偏上的焊缝成形质量比焊枪指向偏下的焊缝成形质量要差，且上下指向差距很大时使其三焊枪形成的熔池上下分离，容易产生焊趾不齐．

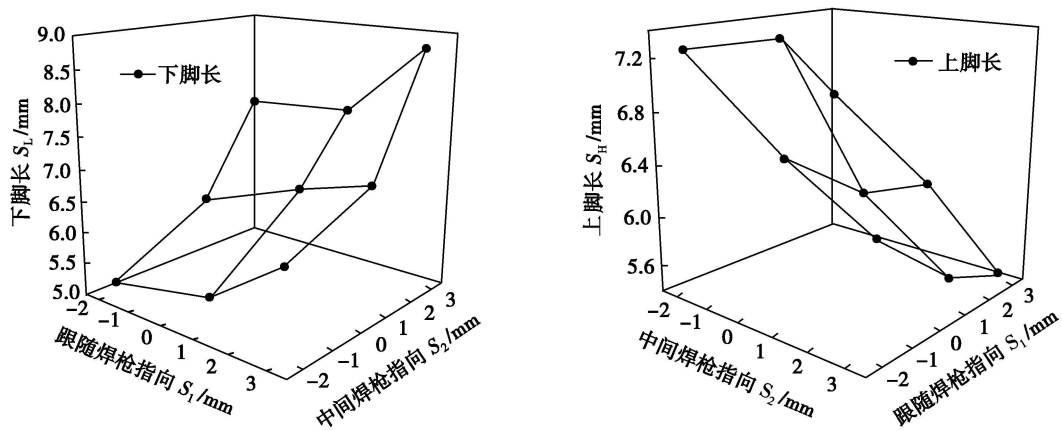

(a) 下脚长与焊枪指向位置关系　　(b) 上脚长与焊枪指向位置关系

图4　不同焊枪指向位置与脚长的关系

Fig. 4　Relationship between electrode offset and leg length

从焊枪左右偏移量试验发现，当左右焊枪偏移量为 ±30 mm 时，即左右焊枪对中时，脚长和熔宽最小，如图5所示，负号表示左侧焊枪在前的偏移量．另外，随着焊丝之间距离的增大，脚长和熔宽逐渐减小，余高随焊丝距离增大而增大．这是因为，焊丝距离增大，两侧的三个热源之间的相互热叠加作用减小，使金属的熔化量相对减小，从而使焊缝成形参数减小，如图6所示．

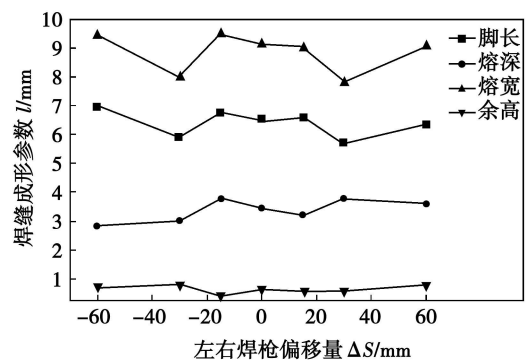

图5　不同左右焊枪偏移量与焊缝成形参数关系

Fig. 5　Relationship between electrode shift and weld geometry parameters

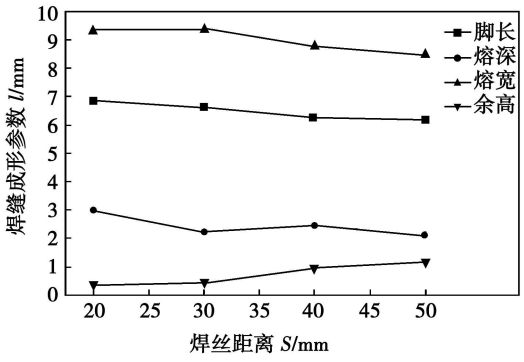

图 6 不同焊丝距离与焊缝成形参数关系

Fig. 6 Relationship between wire to wire distance and weld geometry parameters

3 结 论

(1) 对于 PNP 与 NPN 两种极性组合的焊接, 脚长的平均值均为 6 mm 左右, 可认为两种极性组合时脚长相差不大.

(2) 随着速度的减慢和焊接工艺参数组合的增大, 脚长、熔深和熔宽呈增大趋势. 热源沿焊接方向上的拉长, 焊道最宽处熔宽增大, 可获得良好的焊缝成形.

(3) 下脚长、上脚长受中间焊枪的指向位置影响更为明显. 焊脚长度有一个最大值的限制, 过于偏上焊缝成形质量差, 容易产生脚趾不齐的缺陷.

(4) 当焊枪偏移量为30 mm时, 即左右焊枪对中时, 脚长和熔宽最小.

(5) 随着焊丝之间距离的增大, 脚长和熔宽逐渐减小, 而余高逐渐增大, 距离增大使热源之间的相互叠加作用减小, 从而焊缝成形参数减小, 但这种差别并不显著.

参考文献:

[1] Arita H, Morimoto T, Nagaoka S, *et al*. Technical development of advanced 3-electrode MAG high speed horizontal fillet welding process [C] // The 59th Annual Assembly of the International Institute of Welding. Quebec city, Canada: IIW Commission, 2006, 8: 92—95.

[2] 马晓丽, 华学明, 林 航, 等. 三电极 MAG 高速角焊焊接工艺实验研究[J]. 热加工工艺, 2008, 37(17): 102—104.
Ma Xiaoli, Hua Xueming, Lin Hang, *et al*. Research on triple-electrode high speed MAG fillet welding process [J]. Hot Working Technology, 2008, 37(17): 102—104.

[3] 华学明, 马晓丽, 林 航, 等. 高速三丝熔化极气保护焊接工艺[J]. 焊接学报, 2008, 29(12): 109—112.
Hua Xueming, Ma Xiaoli, Lin Hang, *et al*. Three-wire MAG high speed welding process [J]. Transactions of the China Welding Institution, 2008, 29(12): 109—112.

[4] Iancaster J F. The physics of welding [M]. Oxford: Pergamon Press, 1984.

[5] 冯 雷. 高速 CO_2 焊成形机理与成形稳定性研究[D]. 哈尔滨: 哈尔滨工业大学博士论文, 1999.

作者简介: 马晓丽, 女, 1981 年出生, 博士研究生. 主要从事高效焊接工艺及相关理论的研究工作. 发表论文 3 篇.

Email: mxl@sjtu.edu.cn

and the weld metal is macroscopically separated into one Fe-rich part and one Cu-rich part. Fe-rich phase is filled in the welding line. At the same time, tensile strength of the welded joint is up to 520 MPa, impact toughness is 32.1 J/cm^2, and surface hardness is also close to HB360, which indicates this technology can meet the need of repair of metal parts in field.

Key words: manual self-propagating high-temperature synthesis welding; material; structure; property

Ultrasonic testing of spot weld based on spectrum analysis and artificial neural network CHEN Zhenhua[1], SHI Yaowu[1], ZHAO Haiyan[2] (1. School of Materials Science and Engineering, Beijing University of Technology, Beijing 100022, China; 2. Department of Mechanical Engineering Tsinghua University, Beijing 100084, China). p 76—80

Abstract: The spectrum of testing signal for the spot weld test is analyzed and the characteristic vector which can indicate the characteristics of the signal spectrum of ultrasonic signals for spot weld is obtained. Through using the vector as input data, an artificial neural network is proposed to classify the resistance spot welds in the different diameter level. The testing method proposed in the paper has the advantages of higher recognition ability, higher efficiency and smaller interference factors compared to the traditional methods.

Key words: resistance spot weld; ultrasonic testing; artificial neural network; characteristic vector

Effect of arc atmosphere on interaction of CO_2 laser beam and TIG arc WU Shikai, XIAO Rongshi, ZHANG Huanzhen (Institute of Laser Engineering, Beijing University of Technology, Beijing 100022, China). p 81—85

Abstract: Laser-arc hybrid welding process is closely related to the arc atmosphere. By using a laser power meter, a beam quality diagnosis instrument and a high speed camera, the beam and arc characteristics were investigated during the vertical interaction between a CO_2 laser beam and a TIG arc in argon and helium atmosphere comparatively. The experimental results demonstrate that the laser power attenuates dramatically, the beam defocuses and the beam quality is seriously worsened while the arc voltage drops, the arc column expands, and even combustion wave supported by a laser generates in argon atmosphere. However, the beam and arc characteristics seldom change during the laser-arc interaction in helium atmosphere. The difference of the laser-arc interaction results from the great difference of the electrons number density due to the difference of the gas ionization energy. The electrons number density in the helium arc is 10 times less than that in the argon arc, and thus the inverse bremsstrahlung absorption coefficient of the helium arc is two orders of magnitude lower than that of the argon arc. Meanwhile, there is less difference of the refractive index between the helium arc and the air, so there is no obvious refraction of the helium arc to the laser beam.

Key words: CO_2 laser; TIG arc; arc atmosphere; inverse bremsstrahlung absorption; refraction

Microstructure of cementite beside interface in 321/Qd370qD explosive welding WANG Yufei[1], ZHANG Jinmin[2], YUE Zonghong[2], ZHOU Hao[2], HAN Shunchang[2], SONG Lin[3] (1. School of Materials Science and Engineering, Henan University of Science and Technology, Luoyang 471003, China; 2. Luoyang Ship Material Research Institute, Luoyang 471039, China; 3. Scivic Engineering Corporation, Luoyang 471039, China). p 86—88

Abstract: Cementite near the interface in 321/Qd370qD explosive welding is analyzed by transmission electron microscopy. The results show that there is a lot of cementite in austenitic side of the interface, and a lot of sub-lamellae exist in the cementite beside the interface. These sub-lamellae are about several nanometers and parallel each other. Some sub-lamella groups cross approximately 70.5° and accord with definite crystal tropism relation, which coincide each other when they circumrotate 180° with $[110]_\alpha$ as axis or with $[002]_\alpha$ as axis. Thus, a new sub-lamella group can easily grow beside another sub-lamella group. The crystal tropism relation of adjacent sub-lamellae may be applied to adjacent pearlite groups that maybe exist the above relation.

Key words: explosive welding; cementite; transmission electron microscopy; pearlite

Corrosion resistance of X80 pipeline steel heat-affected zone in S^{2-} medium BI Zongyue[1,2], Lei Ali[1], WANG Na[1], FENG Lajun[1] (1. School of Materials Science and Engineering, Xi'an University of Technology, Xi'an 710048, China; 2. Baoji Petroleum Steel Pipe Co., Ltd, Shan'xi, Baoji 721008, China). p 89—92

Abstract: A three-electrode electrochemistry method is adopted to research the corrosion resistance of heat-affected zone for X80 pipeline steel welding joint prepared by two welding wires (H06H1 and H05MnNiMo) in the Na_2S solution. The results show that the metallurgical structure of the weld heat-affected zone is needle-like ferrite and granular bainite, and the crystal grain is petty. The corrosion rate of the heat-affected zone increases as the raise of Na_2S concentration and temperature, which the corrosion speed is 0.24—0.81 mm/a when the temperature is 20—60 ℃ and the concentration of Na_2S is 1.0%—2.0%, and the corrosion procedure is the anodic polarization of corrosion system; the corrosion procedure is anodic diffusion when the temperature is above 40 ℃.

Key words: pipeline steel; X80 steel grade; welding heat-affected zone; S^{2-} corrosion

Effects of welding conditions on weld geometry parameters for triple-electrode high-speed CO_2 fillet welding on double sides MA Xiaoli[1], HUA Xueming[1], LIN Hang[1], WU Yixiong[1], Yasuhiko ONIKI[2], Shigeru KAMIFUJI[2], SHI Jiangang[2] (1. Shanghai Key Laboratory of Materials Laser Processing and Modification, Shanghai Jiaotong University, Shanghai 200240, China; 2. Tsuneishi Holdings Corporation, Hiroshima 7200393, Japan). p 93—96

Abstract: In order to improve the welding efficiency, triple-electrode high-speed CO_2 fillet welding process was adopted based on the twin-electrode CO_2 welding, and the effect of welding conditions on weld geometry parameters was analyzed. The results show that weld geometry parameters are more or less the same by DCEP/DCEN/DCEP and DCEN/DCEP/DCEN polarities. Leg length, penetration and weld width increase with the speed slowdown and welding combination parameters increase, but leg length has a maximum limit. Middle-electrode offset plays an important role in welding geometry parameters, and the leg length is the smallest when the electrodes shift from one side to the other side is ± 30mm in this experiments. In addition, the leg length and weld width gradually decrease with increasing the distance of wire to wire.

Key words: triple-electrode high speed CO_2 fillet welding; polarities; electrodes shift; weld geometry parameters

Elimination and evaluation of welding residual stress in sterilizers welded by combined process ZHANG Yiliang[1], LIU Jinyan[1], ZHAO Erbing[2], XU Xuedong[1], CHENG Hongwei[2] (1. Beijing University of Technology, Beijing 100124, China; 2. Chaoyang Special Equipment Inspection Institute of Beijing, Beijing 100021, China). p 97—101

Abstract: Observing that cracks appear simultaneously on multi-location near weld on intracavity of domestic vacuum, we investigate a series of studies on welding residual stress and its corresponding elimination methods. We design seven types of combined-structure plates and quantitatively measure the residual stress distribution by X-ray method based on the characteristics of discontinuous welding of different steel in sterilizers. The results show that welding residual stress of all seven types of boards reaches yield stress and causes the stress corrosion and corrosion fatigue which are main reasons of the intracavity cracking of sterilizers. In addition, residual stress resulted from carbon dioxide welding is 10%—22% higher than manual welding, and residual stress is indifferent with rebar type. After experimental verification of post-welding watering quick-cooling technology to eliminate the residual stress, we conclude that watering quick-cooling can effectively reduce the surface residual stress by 50%—70% and increase fatigue limit by 12%—14% on watering surface. Reducing welding residual stress is an important way to solve the problem of cracking in the intracavity of sterilizers.

Key words: weld; residual stress; X-ray method; sterilizer; crack

Character analysis of negative polarity weak plasma arc overlaying welding LIU Zhengjun, YANG Yang, ZHAO Qian, ZHANG Shixin (School of Material Science and Engineering, Shenyang University of Technology, Shenyang 110178, China). p 102—104

Abstract: The essential characteristics of overlaying welding, the influence of the flow and content of protective air on energy density, the arc radial pressure distribution, the heat distribution of plasma arc, the combustion stability and static characteristic of negative polarity weak plasma arc are analyzed. The results indicate that the arc pressure of negative polarity weak plasma arc is homogeneous, the radial distribution graph of arc voltage, the radial distribution graph of arc current and the distribution area of cathode spot all have saucer shape, the energy of cathode spot takes up 50% than that of the effective energy, 90% of the current distributes in the annular area of internal diameter of 10 mm, and changing the flow capacity of protective air can control energy density. The catelectrode atomising action of negative polarity weak plasma arc can effectively improve the combine condition of overlaying metal and basal metal, which makes negative polarity weak plasma arc be one of the perfect thermal resource at dissimilar material overlaying welding.

Key words: negative polarity; weak plasma arc; arc energy; arc pressure

In-situ detection of weld metal thermal cycle of 10CrMo910 steel HU Yanhua, CHEN Furong, XIE Ruijun, LI Haitao (College of Materials Science and Engineering, Inner Mongolia University of Technology, Hohhot 010051, China). p 105—107

Abstract: 10CrMo910 steel was welded by using proper parameters for solving the problem of cold crack and local hardening in the weld or adjacent metal weld of 10CrMo910 steel. Thermo-couples were laid in welded seam during welding to record temperatures in situ, and in-situ detection of thermal cycle about weld metal was realized. The detected maximum temperature during thermal process was 1701℃ and above 401 ℃ than the reported results about heat-affected zone. The welding thermal cycle curves with oil-cooled, air-cooled and sand-cooled for different cooling rates of welded joint were obtained.

Key words: weld metal; welding thermal cycle; in-situ detection

Research status analysis of electron beam welding for joining of dissimilar materials FENG Jicai, WANG Ting, ZHANG Binggang, CHEN Guoqing (State Key Laboratory of Advanced Welding Production Technology, Harbin Institute of Technology, Harbin 150001, China). p 108—112

Abstract: Electron beam welding (EBW) in the field of joining dissimilar materials has been a subject of interest in recent years based on special features of EBW, e. g. high energy density, accurately controllable beam size and location, low residual stress and pollution-free weld. Numerous successful results have been achieved, and some of them have already been exploited in industrial production. Since EBW is a fusion welding method, difficulties associated with metallurgical phenomena still exist. This paper is aimed to have an analysis of the research status of electron beam welding for the joining of dissimilar materials. A summary of the existing problems and solutions during electron beam welding of different type of dissimilar material joint has been conducted and the key points of research in future are also proposed.

Key words: dissimilar materials; electron beam welding; research status